Available online at www.sciencedirect.com

SciVerse ScienceDirect

Procedia Engineering 32 (2012) 291 – 298

Procedia Engineering

www.elsevier.com/locate/procedia

I-SEEC2011

Force Sensing Device Design using a Modified Add-Drop filter

K. Kulrod[a*], C. Sirawattananon[a], S.Mitatha[a], K. Srinuanjan[b], P.P. Yupapin[b]

[a]*Hybrid Computing Research Laboratory (HCRL), Faculty of Engineering*
[b]*Nanoscale Science and Engineering Research Alliance (N'SERA), Faculty of Science*
King Mongkut's Institute of Technology, Ladkrabang(KMITL), Bangkok 10520, Thailand

Elsevier use only: Received 30 September 2011; Revised 10 November 2011; Accepted 25 November 2011.

Abstract

We propose a new sensing device using a modified add-drop filter known as a PANDA ring resonator type, in which the sensing unit is consisted of an optical add/drop filter and two nanoring resonators, where one ring is placed as a sensing device, the other ring is set as a reference. In operation, the external force is assumed to exert on the sensing ring resonator, which can form the measurement. The finite difference time domain (FDTD) method called Optiwave is used to manipulate the sensing behaviors of the proposed system. The obtained results have shown that the change in wavelength due to the change in sensing ring radii is seen, in which the wavelength shift of 1 nm resolution is achieved. The recovery and the reciprocal signals can also be formed, which can be used to approach to many advantages of measurements, including the possibility of standardizing measurement accuracy. The behavior of light within a PANDA ring resonator is also analyzed and reviewed.

Keywords: Force sensor; Optical sensor; Self calibration

1. Introduction

In the recent years, optical sensors have been implemented and widely used in various applications, for instance, in medicine, microbiology, communication, particle physics, automotive, environmental safety and defense [1-3]. Particularly, the integrated nonlinear optical device using a microring resonator has been widely investigated in both theory and experiment [4-6]. It can be used as sensors to measure force, strain, temperature, pressure and other quantities by modifying an optical device so that the quantity to be

* Mr. Kritsada Kulrod. Tel.: +66-2-329-8341; fax: +66-2-329-8343.
E-mail address: yoyona_ja@hotmail.com.

doi:10.1016/j.proeng.2012.01.1270

measured modulates the intensity, phase, polarization and wavelength or transit time of light in the waveguide. One of the interesting results is the use of a specific model of a modified add-drop filter known as a PANDA ring resonator [7], which can be a good candidate for force sensing device. Especially it have a numerous advantageous features such as small size, ruggedness, potential for realizing various optical functions on a single chip (integration with other optical components), multi-channel sensing, etc. The use of force measurement with more efficiency systems has been reported by several research groups [8, 9]. Recently, the use of a new form of a PANDA ring resonator has shown the interesting aspect of applications [10, 11], where the authors have shown that such a proposed form of a ring resonator can establish the new concept of dark-bright soliton conversion, whereas the use of random encoding, optical vortices (tweezers) and optical/quantum gate can be generated.

In this paper, we present the use of a PANDA ring resonator, which can be employed as a force sensing application, in which the resolution in the range of *nN* (nano Newton) can be achieved by measuring the wavelength shift, moreover, the low power consumption due to the low intensity source is the other advantage. The sensing system is functioned by mean of the change of a ring radius due to a load cell or other physical parameters, in which the change in optical path length of light is caused by the same way of an interferometer [12, 13], while the other ring radius remain constant(reference signal). The sensing and the reference signals are analyzed, simulated and compared to form the measurement. Simulation results obtained have shown that the system can be employed to be a force sensing at nanoscale. However, the measurement limitation due to wavelength meter resolution and material elongation limit is occurred, in which the measurement resolution of 1 nm is noted in this work and the interesting results are the self-calibration sensor base on ring resonator is discussed in details.

2. Modified Add-Drop filter

To form the simulation sensing performance, the microring material used is *InGaAsP/InP*, with the refractive index is n_0 = 3.34 [14-16]. The schematic diagram of a sensing system using a PANDA ring resonator is as shown in Fig. 1. The system is consisted of three microring resonators, where the first ring is placed as a reference ring, with radius R_1 = 1.550 μm. The second ring R_2 is the sensing ring, the ring radii are varied from 1.550 – 1.558, and the third ring is used to form the interference signal between reference and sensing rings, with the radius R_3 is 3.10 μm. In operation, the change in sensing ring radius is caused by the change in the shift of signals circulated in the interferometer ring (R_3), in which the interference signal is seen. The change in optical path length which is related to the change of the external parameters is compared and measured.

Two identical beams of monochromatic optical field (E_{in}) of Gaussian pulse with the center wavelength at 1.550 μm are launched into in the system at the input and the add ports, respectively, which is given by

$$E_{in}(t) = E_0 \exp\left[-\alpha L + j\phi_0(t)\right]. \quad (1)$$

Here E_0 is constant light source amplitude, $L = 2\pi R$ is a propagation distance (waveguide length), α is an attenuation coefficient and ϕ_0 is the phase constant. When light propagates within the nonlinear material (medium), by considering the Kerr nonlinear effect within the ring devices, the refractive index (n) of light within the medium is given by

$$n = n_0 + n_2 I = n_0 + \frac{n_2}{A_{eff}} P \tag{2}$$

Here n_0 and n_2 are the linear and nonlinear refractive indices, respectively. I and P are the optical intensity and optical power, respectively. The effective mode core area of the device is given by A_{eff} .

The resonance output is formed, thus, the normalized output of the light field is the ratio between the output ant input fields $\left[E_{out}(t) \text{ and } E_{in}(t)\right]$ in each round trip, which is given by [4, 7]

$$\left|\frac{E_{out}(t)}{E_{in}(t)}\right|^2 = (1-\gamma)\left[1 - \frac{\left(1-(1-\gamma)x^2\right)\kappa}{\left(1-x\sqrt{1-\gamma}\sqrt{1-\kappa}\right)^2 + 4x\sqrt{1-\gamma}\sqrt{1-\kappa}\sin^2\left(\frac{\phi}{2}\right)}\right] \tag{3}$$

The optical output of ring resonator add/drop filter for the through and drop port can be given by equations (4) and (5), respectively [7]

$$\left|\frac{E_{t1}}{E_{in}}\right|^2 = \frac{(1-\kappa_1) - 2\sqrt{1-\kappa_1}.\sqrt{1-\kappa_2}.e^{\frac{-\alpha}{2}L}\cos(k_n L) + (1-\kappa_2)e^{-\alpha L}}{1 + (1-\kappa_1)(1-\kappa_2)e^{-\alpha L} - 2\sqrt{1-\kappa_1}.\sqrt{1-\kappa_2}e^{\frac{-\alpha}{2}L}\cos(k_n L)} \tag{4}$$

$$\left|\frac{E_{t2}}{E_{in}}\right|^2 = \frac{\kappa_1\kappa_2.e^{\frac{-\alpha}{2}L}}{1 + (1-\kappa_1)(1-\kappa_2)e^{-\alpha L} - 2\sqrt{1-\kappa_1}.\sqrt{1-\kappa_2}e^{\frac{-\alpha}{2}L}\cos(k_n L)} \tag{5}$$

Here E_{t1} and E_{t2} represent the optical fields of the through and drop ports, respectively. $x = \exp\left(-\alpha L/2\right)$ is a round trip loss coefficient, $k_n = 2\pi/\lambda$ is the wave propagation number in vacuum, n_{eff} is an effective refractive index, $\phi = k n_{eff} L$ is the phase constant, γ is the fractional coupler intensity loss, κ is the coupling coefficient, and β is a complex coefficient, The signals of both rings R_1 and R_2 are observed at the point Ref.1 (E_{R1}) and Sen.1 (E_{S1}) respectively as shown in Fig. 1, and the mathematical forms of those signals are also analyzed, which can be expressed as

$$\left|\frac{E_{S1}}{E_{in}}\right|^2 = \left|\left[\frac{-(1-\gamma_S)\kappa_S}{1 - Z_2(1-\gamma_S)(1-\kappa_S)}\right].\left[\frac{j\,.\,Z_3\sqrt{(1-\gamma_C)\kappa_C}\left(1 + Z_3^2\beta_1\sqrt{(1-\gamma_C)(1-\kappa_C)}\right)}{1 - Z_3^4\beta_1\beta_2(1-\gamma_C)(1-\kappa_C)}\right]\right|^2 \tag{6}$$

$$\left|\frac{E_{R1}}{E_{in}}\right|^2 = \left[\frac{-(1-\gamma_R)\kappa_R}{1-Z_1(1-\gamma_R)(1-\kappa_R)}\right]\left[\frac{j\,.\,Z_3\sqrt{(1-\gamma_C)\kappa_C}\left(1+Z_3^2\beta_2\sqrt{(1-\gamma_C)(1-\kappa_C)}\right)}{1-Z_3^4\beta_1\beta_2(1-\gamma_C)(1-\kappa_C)}\right]^2 \quad (7)$$

Here E_{S1} and E_{R1} represent the sensing and reference signal respectively, γ_S and γ_R are the fractional coupler intensity loss in sensing and reference unit, κ_S and κ_R are the coupling coefficient in sensing and reference unit,

$Z_1 = \exp\left(\frac{-\alpha}{8}\frac{L_1}{2} - jk_n\frac{L_1}{2}\right)$, $Z_2 = \exp\left(\frac{-\alpha}{8}\frac{L_2}{2} - jk_n\frac{L_2}{2}\right)$ and $Z_3 = \exp\left(\frac{-\alpha}{8}\frac{L_3}{4} - jk_n\frac{L_3}{4}\right)$ are loss coefficients, and β is a complex coefficient, which they are described by

$$\beta_1 = \left[\frac{\sqrt{(1-\gamma_3)(1-\kappa_3)} + (1-\gamma_3).e^{\frac{-\alpha L_1}{4} - jk_nL_1}}{1-\sqrt{(1-\gamma_3)(1-\kappa_3)}.e^{\frac{-\alpha L_1}{4} - jk_nL_1}}\right] \quad (8)$$

$$\beta_2 = \left[\frac{\sqrt{(1-\gamma_0)(1-\kappa_0)} + (1-\gamma_0).e^{\frac{-\alpha L_2}{4} - jk_nL_2}}{1-\sqrt{(1-\gamma_0)(1-\kappa_0)}.e^{\frac{-\alpha L_2}{4} - jk_nL_2}}\right] \quad (9)$$

The power output P at sensing port E_{S1} is expressed by

$$P = \left|E_{S1}\right|^2 \quad (10)$$

The power output P at reference port E_{R1} is expressed by

$$P = \left|E_{R1}\right|^2 \quad (11)$$

To compare the reference and sensing signals, we set $\gamma_0 = \gamma_3$, $\kappa_0 = \kappa_3$ so $\beta_1 = \beta_2$ and then set $\gamma_S = \gamma_R$, where finally E_{S1} and E_{R1} are both identical if $L_1 = L_2$. Then E_{S1} is varied while L_2 is changed by means of varying R_2 with respect to E_{R1}, in which R_2 remains constant. By using the finite difference time domain method (FDTD), the system is analyzed by using the computer programming called Opti-wave, whereas all parameters are simulated based on the practical parameters. The simulation steps are 40,000 iterations and the peak spectrum at point Ref.1 and Sen.1 are set as reference and sensing signals respectively, as shown in Fig. 2 and 3. The change in optical path length between sensing and reference signals is compared, in which the induced change by the external parameters is measured.

This measurement is formed by the comparison of the shift in wavelength (optical path length), i.e. wavelength shift ($\Delta\lambda$) is given by

$$\Delta\lambda = \lambda_2 - \lambda_1 \tag{12}$$

Here λ_1 and λ_2 are the peak wavelengths of Ref.1 and Sen.1, respectively. The relationships between intensity and wavelength-shift are plots as shown in Fig. 3.

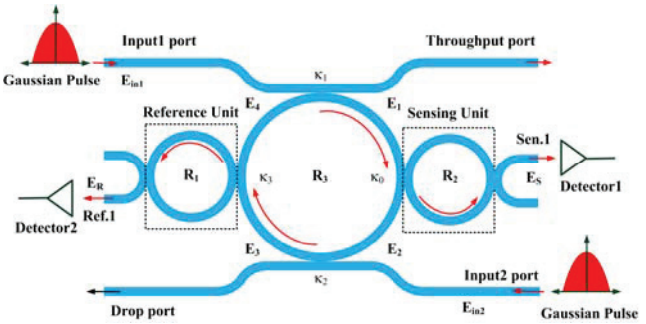

Fig. 1. Schematic diagram of a nano-scale sensing transducer using PANDA ring resonator

3. Force Sensing Operation

In simulation, the sensing ring radius R_2 is varied from 1.550 to 1.558 μm, in which the optical path length is also changed, and an interferometer system is formed [12, 13]. Both signals, sensing and reference signals are observed and compared, and the measurement is formed [8, 9]. We assume that the load cell or other sensing parameters can exert on the second ring R_2, whereas stress and strain are introduced on the sensing device by means of the elastic modulus of the materials, which is caused the difference in peak spectrum of both signals and described by equation (13)

$$Y_0 = \frac{F/A}{\Delta L/L} = \frac{Stress}{Strain} \tag{13}$$

The relationship between force and the change in sensing device length is described by

$$F = \left(\frac{Y_0 A_0}{L_0}\right).\Delta L \tag{14}$$

Where F is the applied force, Y_0 is the Young modulus, A_0 is the initial cross-section area, L_0 is the initial length and ΔL is the change in length. According to the property of InGaAsP/InP material [14-16], the relationship between force and wavelength shift is plotted as shown in Fig. 4.

By using equation (14) and the simulation results in Figs. 2 and 3, the relationship between Force and Wavelength-shift of the reference and sensing signals is as shown in Fig. 4. In this case, the nano forces are ranged between 0.0 and 16.0 *nN*, which are caused by the coupling effects between the sensing device and the surrounded environment, for instance, molecule, DNA or atom. We found that a sensing range in terms of wavelength-shift ($\Delta\lambda$) within the resolution of 1 nm is achieved. Fig. 3 shows the relationship between the varying ring radius R_2 and the wavelength-shift ($\Delta\lambda$) by comparing the sensing and reference signals, where the self-calibration is formed. By using the least square curve fitting, the linearity relationship between the applied force and wavelength shift with R^2 = 0.9823 is formed, which is shown

in good linearity for sensing application. In addition, when force is applied on the sensing ring, where the change in resonance frequency i.e., the free spectral range (FSR) is introduced, in which the ring radii R_2 are varied from 1.550 to 1.558 μm. However, when the applied force is larger than 16.0 nN the measurement limitation is occurred due to the elastic limit of the sensing material, where the plot of the relationship between force and wavelength shift is no more linear.

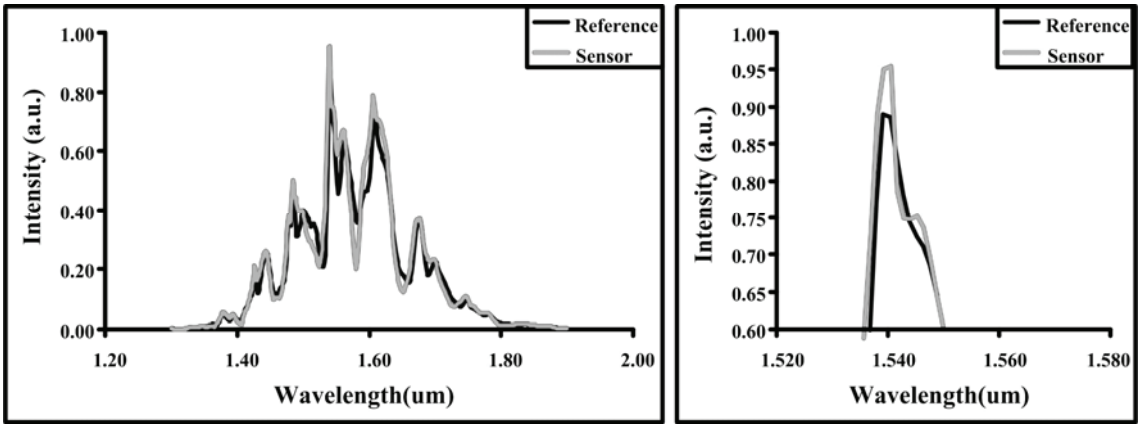

Fig. 2. Shows the relationship between intensity and wavelength of sensing (E_{S1}) and reference signals (E_{R1}), with the radius R_1 (black line) and R_2 (gray line) = 1.550 μm

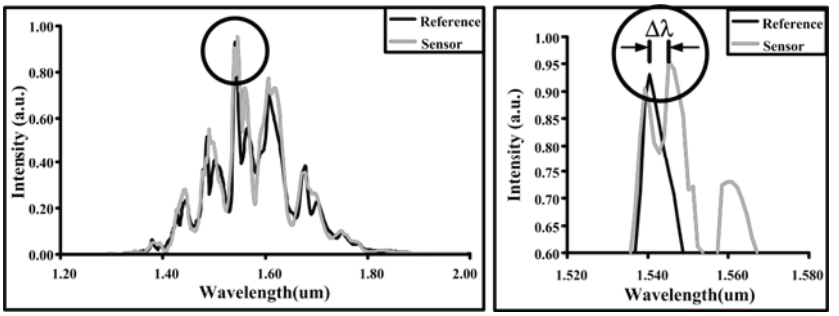

(a) R_1 (black line) = 1.550 μm and R_2 (gray line) = 1.552 μm

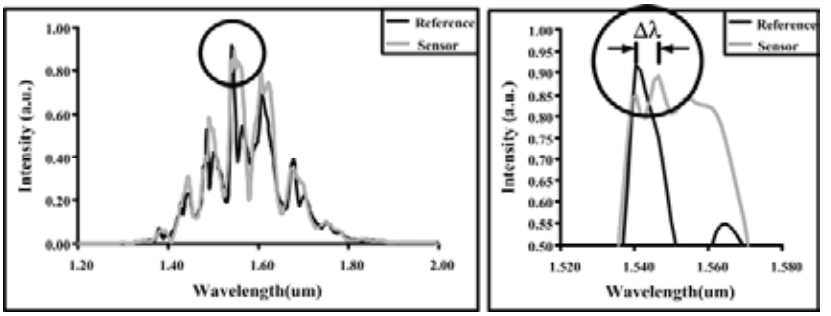

(b) R_1 (black line) = 1.550 μm and R_2 (gray line) = 1.554 μm

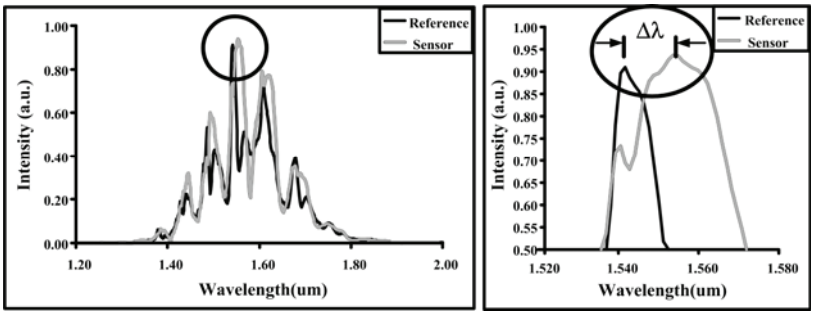

(c) R_1 (black line) = 1.550 μm and R_2 (gray line) = 1.556 μm

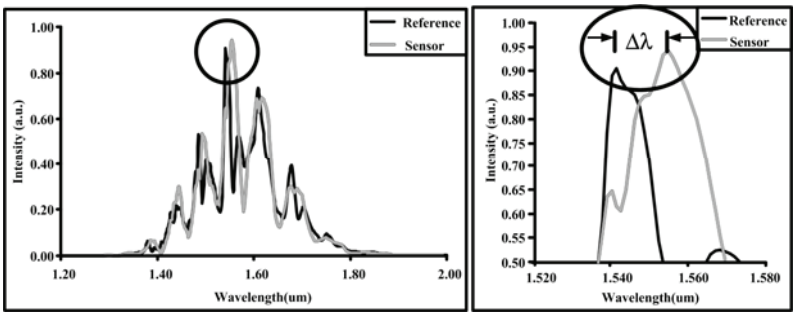

(d) R_1 (black line) = 1.550 μm and R_2 (gray line) = 1.558 μm

Fig. 3. Shows the relationship between intensity and wavelength of sensing (E_{S1}) and reference signals (E_{R1}), with the radius R_1 (blue line) = 1.550 μm and R_2 (red line) is varying form 1.552-1.558 μm, (a) R_2 = 1.552 μm, (b) R_2= 1.554 μm, (c) R_2 = 1.556 μm, and (d) R_2 = 1.558 μm

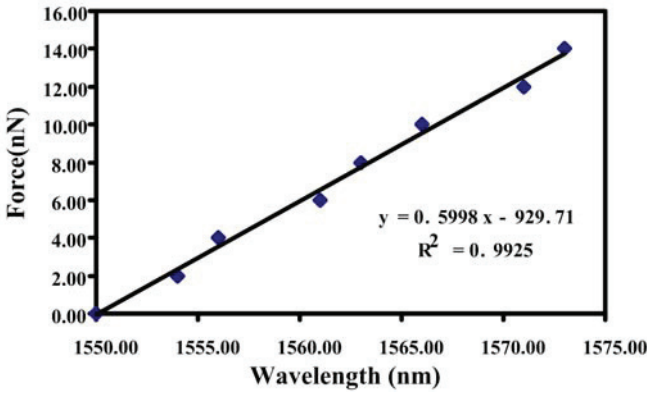

Fig. 4. Graph of the linear relationship between Force and the Wavelength

4. Conclusion

We have proposed the system of a force sensing system using PANDA ring resonator to make the benefit of the accuracy of measurements in nano-scale measurement range and the measurement resolution of 1 nm is obtained. The calibration is allowed by using the change in wavelength between sensing and reference signals, which is existed within the system. The self-calibration of the measurement

between sensing and reference signals can be compared without any additional optical part or other addition unit. The other advantage of the proposed system is the remote measurement, which is also available due to the use of the integrated optic device.

References

[1] E. Sifuentes, O. Casas, and R. Pallas-Areny, "Wireless Magnetic Sensor Node for Vehicle Detection With Optical Wake-Up", IEEE Sensors Journal, vol. 11(8), pp. 1669-1676, 2011.
[2] C. R Dennison, P. MWild, D. R Wilson and M. K Gilbart, "An in-fiber Bragg grating sensor for contact force and stress measurements in articular joints", Measurement Science and Technology, 21(11), 2010.
[3] A. Grillet, D. Kinet, J. Witt, M. Schukar, K. Krebber, F. Pirotte and A. Depre, "Optical fiber sensors embedded into medical textiles for healthcare monitoring," IEEE Sensors Journal, vol. 8(7), pp.1215-1222, 2008.
[4] Y.G. Boucher and P. Feron, "Generalized transfer function: A simple model applied to active single-mode, microring resonators", Optics Communications, vol. 282(19), pp. 3940–3947, 2009.
[5] L. Jin, M. Li and J.-J. He, "Highly-sensitive optical sensor using two cascaded-microring resonators with Vernier effect", ACP 2009, 2009.
[6] M. Huang, J. Yang, S. Jun, S. Mu and Y. Lan, "Simulation and analysis of a metamaterial sensor based on a microring resonator", Sensors, vol. 11(6), pp. 5886-5899, 2011.
[7] K. Uomwech, K. Sarapat, and P.P. Yupapin, "Dynamic modutated Gaussian pulse propagation within the double PANDA ring resonator system", Microwave and Optical Technology Letters, vol. 52(8), pp. 1818-1821, 2010.
[8] H. Kim, T. Song, and K.-H. Ahn, "Sharply tuned small force measurement with a biomimetic sensor", Applied Physics Letters, vol. 98(1), 2011.
[9] M. Suzuki, G. Kawai, H. Izumi, S. Aoyagi and S. Yokoyama, "Design and simulation of inertial force sensor using mach-zehnder interferometer with optical waveguides made of crystal silicon", IEEJ Transactions on Sensors and Micromachines, vol.129(9), pp. 301-306, 2009.
[10] P. Juleang, P. Phongsanam, S. Mitatha and P.P. Yupapin, "Public key suppression and recovery using a PANDA ring resonator for high security communication", Optical Engineering, vol. 50(3), 2011.
[11] T. Phatharaworamet, Chat Teeka, R. Jomtarak, S. Mitatha and P.P. Yupapin, "Random binary code generation using dark-bright soliton conversion control within a PANDA ring resonator," IEEE J. Lightwave Technology, vol. 28(19), pp. 2804-2809, 2010.
[12] N. K. Berger, "Measurement of subpicosecond optical waveforms using a resonator-based phase modulator", Optics Communications, vol. 283(7), pp. 1397-1405, 2010.
[13] P. Hua, B.J. Luff, G. R. Quigley, J. S. Wilkinson, K. Kawaguchi, "Integrated optical dual Mach–Zehnder interferometer sensor", Sensors and Actuators, B:Chemical, vol. 87(2) pp. 250-257, 2002.
[14] M. Levinshtein, S. Rumyantsev, M. Shur, "Handbook Series on Semiconductor Parameters", World Scientific, 1, 147-168(1996).
[15] M. Levinshtein, S. Rumyantsev, M. Shur, "Handbook Series on Semiconductor Parameters", World Scientific, 2, 153-179(1999).
[16] T. P. Pearsall, "GaInAsP Alloy Semiconductors", John Wiley and Sons, 1982.